

Preparation of a Biomass Potential Map

Sönke Müller¹, Torge Steensen², Olaf Büscher¹, Michael Jandewerth³

Abstract

Achieving a fossil-resources-free power supply requires an exploration of alternative, renewable energy sources. Over the last years, biomass has become an important component of this endeavour and its consumption is rising steadily. Common sources of biomass are agricultural production and forestry but the production of these sources is stagnating due to limited space. To explore new sources of biomass, for example in the field of landscape conservation, the location and available amount of biomass must be obtained. Normally, there are no reliable data sources that give information about the objects of interest like hedges and vegetation along streets, railways, rivers and field margins. There is a great demand for an inventory of these biomass sources which could be answered by applying remote sensing technology.

To generate that kind of spatial information, satellite imagery is used in combination with area-wide available GIS and elevation data. The multispectral satellite images are assumed to have a low spatial resolution of 10-20 m and spectral bands corresponding to the Sentinel-2 spatial and spectral configurations. For GIS data, the German Digital Landscape Model (ATKIS Base-DLM), containing roads, field boundaries and waterways, supports the mapping allowing for deduction of potential biomass objects located beside GIS objects. To allow a quantitative estimation of the biomass volume, a digital surface model (DSM), produced from raw LIDAR data, is utilized.

1. Introduction

Renewable energy sources are key components in reducing the consumption of limited fossil fuels. As opposed to coal and gas, the generation of power through solar energy, water, wind or biomass does not unlock carbon dioxide (CO₂) that has been buried in the ground for the last millions of years and, hence, does not effectively add CO₂ to the atmosphere in the medium to long term. Because of this lack of net-created CO₂, research has focused on exploitation of such energy sources over the past years ([3], [5], [6], [8]).

Biomass is a key player in this suite of renewable energies as it is abundant on most land areas and has the potential to re-grow in a few months to years. Prime targets for biomass production are forests and agricultural areas but due to a limited extend of these, alternative vegetation sources need to be identified.

The biomass objects of interest are vegetation stripes alongside streets, railways and waterways, unploughed stripes that separate fields and in general hedgerows (see Figure 1 for examples). The objects have elongated shapes with a limited width in the range of 5 to 20m and can be found in a range of places resulting in a great potential as biomass energy source.

We further separate these types into ligneous, graminaceous and herbaceous vegetation. These sub-categories have an inherent consequence for the growth pattern, hedge type and size of the respective plants and the amount of biomass produced in a given temporal interval.

¹ EFTAS Fernerkundung Technologietransfer GmbH, Oststraße 2-18, 48145 Münster, Germany, {soenke.mueller, olaf.buescher}@eftas.com

² Institute of Photogrammetry and GeoInformation, Leibniz Universität Hannover, Nienburger Str. 1, 30167 Hannover, Germany, steensen@ipi.uni-hannover.de

³ Fraunhofer-Institut für Umwelt-, Sicherheits- und Energietechnik UMSICHT, Osterfelder Str. 3, 46047 Oberhausen, Germany, michael.jandewerth@umsicht.fraunhofer.de

The maintenance of these biomass objects works normally as follows: vegetation alongside streets is trimmed to keep a special shape that allows traffic to pass while vegetation alongside fields is sometimes maintained by farmers but in most cases very irregular. A central collection system of the accruing biomass only exists in few areas. The approach presented here will address that point.

To estimate the biomass potential of these areas, a detailed map of the amounts of vegetation is required. As no local information is available, we use a combination of low-cost data sources to calculate the necessary information. First, a vegetation height map is created utilising LIDAR data. This map will then be compared to aerial imagery (AISA Eagle), which we have as a substitute for the upcoming Sentinel-2 data. A spectral unmixing of the comparably large pixels (10 to 60 m) is done using the Sequential Maximum Angle Convex Cone (SMACC) approach. With the endmember specifications and the determined vegetation height, we are able to derive the biomass volume. This data, in turn, will allow the analysis of potential regions where the usage of the existing biomass is feasible for energy production.

Our test site is located close to the city of Bottrop in North Rhine-Westphalia, Germany. It comprised a rural area with intensive agricultural use but also contains parts of a natural preserve.



Figure 1: Examples of target objects in test site: vegetation alongside streets (left and middle), unploughed strips (right).

2. Related Work

Normally only agricultural crops and forest vegetation are considered in remote sensing approaches that deal with biomass feedstock production. A good overview about these approaches can be found in [1] where concepts, methods and commercial software are reviewed for the monitoring of energy crops.

However a few approaches are existing that deal with small biomass units in contrast to the common agricultural crop production and forestry. In most cases, additional information is used for these approaches in form of height information in order to increase the recognition rates. In the following some ideas of approaches that deal with small biomass units are reviewed.

A combination of LIDAR data and airborne images to estimate biomass and volume of shrub vegetation is used in [5]. Features of both data sources serve here as input to a regression model. The results show good accordance of the estimations and ground truth data.

The application of a two-stage approach based on spectral information from SPOT satellite images to retrieve an estimation of woody biomass can be found in [6]. In the first stage the author classifies the images with a Maximum Likelihood classifier to find regions of arboreal, shrub and herbaceous vegetation. The second stage of the approach is aimed at finding an analytical model

representing the relationship between vegetation parameters like tree height and stem diameter and the spectral SPOT information by correlation analysis.

An existing known model that estimates the carbon content of single pine trees with tree height and crown diameter as parameters is applied in [8]. In airborne LIDAR data tree crowns are identified with an adaptive technique of Local Maximum Focal Filtering resulting in the two variables necessary for the carbon model.

Considering SAR data, the potential of TerraSAR-X High Resolution Spotlight images to classify grasslands, herbaceous, trees, shrubs and flower strips into different classes is investigated in [3]. The author processes a time series of six images of one year and successfully applies a Random Forest classifier. For woody structures the approach delivers producer's accuracies above 80 %.

3. Strategy and Data Description

3.1. Strategy

In our work, we present an approach dealing with small units of biomass that can be detected using a combination of two data sources. For the first data source, the spectral information, we assume low spatial resolution satellite data of about 10-20 m Ground Sampling Distance (GSD) which has the advantage of being cost-effective and nearly area-wide available. This data source will provide the qualitative identification of vegetated areas.

Although data in the range of 10-20 m GSD exists, our approach aims at using Sentinel-2 data that will be freely available from 2015 and has a setup of 13 spectral bands. Therefore, we simulate corresponding data using measurements from an airborne line scanner with similar spectral bands.

The second source of data is height information in form of digital surface models (DSM). This data can be derived directly from LIDAR acquisitions or through stereo matching of aerial images that are normally widely available. In this secondary data, we are able to quantitatively analyse the vegetation detected earlier in terms of height, volume and mass. For our test site, we use LIDAR data that was acquired synchronously to the line scanner flight.

Both data sources are processed to indicate biomass potential: Spectral unmixing is applied to the spectral data to generate qualitative biomass indicators while the LIDAR data is used to produce a digital surface model as quantitative biomass indicator. Both processing steps are described in detail in the next chapter. The result of the processing is an information layer stack that enables an exact estimation of the biomass amount. In this part of the study, we build the biomass potential map to outline the vegetated areas that can be considered for energy production. The amount estimation, the amount prediction and an economic analysis including logistic aspects will be the topic of follow-up research.

3.2. AISA Eagle

The AISA Eagle sensor is a passive hyperspectral airborne line scanner that works in a spectral range of 400-970 nm and separates, depending on the image rate [images per second], up to 488 spectral bands. For our experiments, a configuration of 107 spectral bands in a range of 431-926 nm with a spatial resolution of 0.5 m is used. The bandwidths in our test dataset of the single bands lie between 4.27 nm and 4.81 nm. The single strips for our test site are preprocessed by the data provider to an image mosaic. The flight height was at 800 m above ground. Sample data is illustrated in Figure 2a.

3.3. LIDAR

Synchronously to the recording of hyperspectral information, a RIEGL LMS-Q680i full waveform laser scanner was used to acquire height information. The height information is delivered in binary LAS file format, a public file format for the interchange of 3-dimensional point cloud data (see [2]). The LAS file format supports up to 15 return pulses per outgoing pulse. The differentiation of the return pulses is important for dealing with vegetation, because vegetation objects typically deliver more than a single return pulse due to the intertwined leaf and branch structure. Sample data is illustrated in Figure 2b.

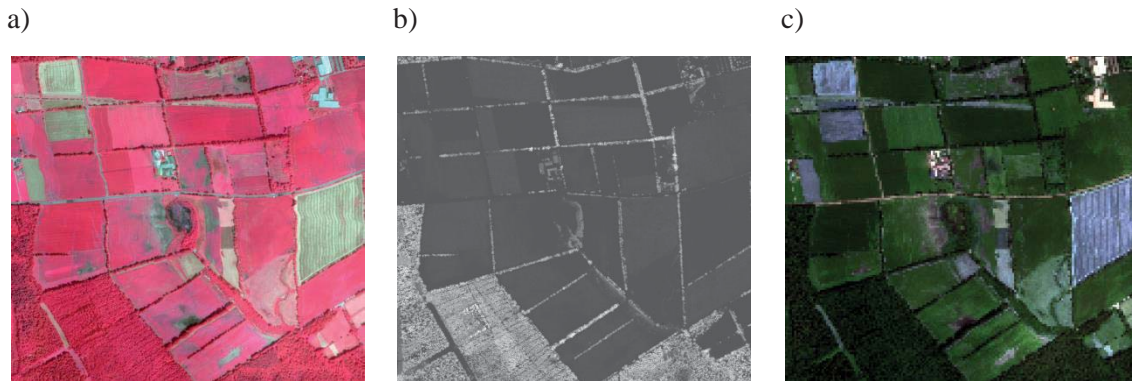


Figure 2: a) CIR bands of AISA Eagle input data b) LIDAR input data c) simulated Sentinel-2 data, 10m GSD

4. Methods

4.1. Vegetation height map

To generate vegetation height information from the raw LIDAR data, a classification into ground and non-ground points on the basis of the recorded return pulses is applied. The procedure works as follows: If the return signal of a single LIDAR point contains more than one return, the first return represents the surface of vegetation and the last pulse represents the ground. If vegetation exists, the height above ground is calculated by building the difference between the first and the last pulse. If a LIDAR point lies on soil or sealed areas the height is set to zero.

Normally LIDAR points are acquired in an irregular distribution, but, for our application, a regular distributed vegetation height is needed to assign a vegetation height to each pixel. To achieve this, all existing LIDAR points are utilised to span a TIN (triangulated irregular network). At the positions of a regular raster, the height values are linearly interpolated to the TIN data set. The LIDAR point cloud we use at our test site is very dense compared to the spectral data, resulting in a negligible interpolation error.

4.2. Sentinel-2 simulation

Sentinel-2 (see [4]) will be a pair of two satellites with the start of the first satellite planned for 2015. Sentinel-2 will deliver data in the visible, near infrared and shortwave infrared spectrum comprising 13 spectral bands: 4 bands at 10 m, 6 bands at 20 m and 3 bands at 60 m spatial resolution, with a swath width of 290 km. Sentinel-2 will be placed in a 5 day repeat-cycle orbit what guarantees a high degree of data availability.

In the following, the simulation procedure of Sentinel-2 data based on a hyperspectral AISA Eagle dataset is described. In comparison to other data simulation approaches (see [9]), where complex sensor models are known and used, a simplified method is applied here.

Firstly, corresponding bands between the source (AISA Eagle) and target dataset (Sentinel-2) are determined. For example, band 1 of Sentinel-2 covers a bandwidth between 433 nm and 453 nm. All AISA Eagle bands that lie in this range, bands 2 to 6, form the basis for the simulation. The complete band mapping is shown in Table 1.

Secondly, pixel values (digital numbers, DN) are calculated for each of the 9 Sentinel-2 simulation bands according to Equation 1, where t_i is the band number of the target dataset, s_n the band number of the source (AISA Eagle) dataset. Afterwards all DN values are normalised to a range between 0 and 1 to compensate the different amount of AISA Eagle bands that lie in the range between 3 and 24 bands.

$$DN_{t_i} = \sum_{n=n_{min}}^{n_{max}} DN_{s_n} \quad (1)$$

Thirdly, a spatial resampling of the simulated bands is done to get the desired target resolution of 10 m, 20 m or 60 m. In Figure 2c, the simulation results for bands 2-4 with a spatial resolution of 10 m are illustrated.

Sentinel-2 simulation data band number	Accumulated AISA Eagle bands	Amount of AISA Eagle bands	Target spatial resolution [m]
1	2-6	5	60
2	8-21	14	10
3	26-33	8	10
4	49-55	7	10
5	60-62	3	20
6	67-69	3	20
7	76-79	4	20
8	78-101	24	10
8b	93-96	4	20

Table 1: Corresponding AISA Eagle bands for Sentinel-2 simulation.

4.3. Spectral unmixing

Due to the limited spatial resolution of the Sentinel-2 simulation data and objects of interest that are smaller than pixel size, the application of multispectral classification at sub-pixel level is limited or difficult. The smallest objects of interest, for example vegetation alongside streets and unploughed strips, have a width of no more than 3 to 5 m. Thus, a single image pixel represents a mixture of reflectance values of several materials.

In contrast to classification methods that assign the most probable class to each pixel, spectral unmixing decomposes a mixed pixel spectrum into a collection of constituent spectra, called endmembers, and a set of corresponding fractions, or abundances. Endmembers represent the reflectance characteristics of pure material reflectances, for example water, soil, vegetation and street surfaces. Spectral unmixing works in two steps: An initial endmember detection followed by the spectral unmixing itself.

For our experiments, a powerful endmember detection approach called Sequential Maximum Angle Convex Cone (SMACC), that is available in the software ENVI, is used. SMACC ([7]) works with

a convex cone model (residual minimization) and selects unsupervised existing endmembers in image data.

SMACC starts with a single endmember and increases incrementally in dimension. The data vector that builds the maximum angle with the existing endmember is taken as additional new endmember and extends the endmember set. The algorithm ends, if the maximum number of found endmembers is reached or if the maximum relative error is below a specific threshold. In Figure 3 on the left hand side, the development of the maximum relative error in relation to the number of endmembers is illustrated. It can be seen that the maximum relative error converges starting from an amount of 4 endmembers.

For the second step, linear spectral unmixing (LSU) is applied that works with a linear mixture model according to Equation 2, where DN is a pixel value, N the number of endmembers, a_i the abundance of endmember i and s_i the spectrum of endmember i . According to Equation 3, the sum of all abundances for a unique pixel has to be 1.

$$DN = \sum_{i=1}^N a_i s_i \quad (2)$$

$$\sum_{i=1}^N a_i = 1 \quad (3)$$

This approach results in abundance maps, the extracted endmember spectra (Figure 3 right) and mapping information about single endmember locations in the image.

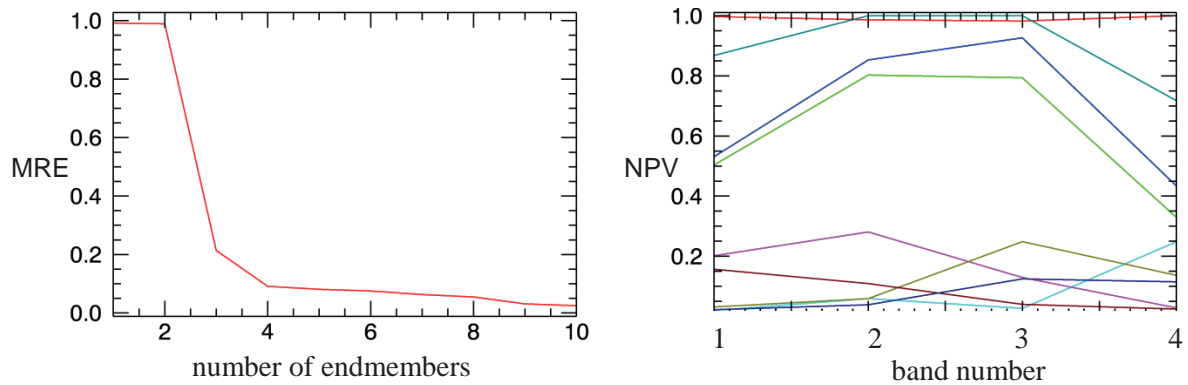


Figure 3: SMACC output, behaviour of the maximum relative error (MRE) according to the number of endmembers (left) normalized pixel values (NPV) of endmember spectra (right).

4.4. Potential map

As final step, the biomass potential map is set up as a multi-layer image of biomass indication information. The map is based on the result of the spectral unmixing and the DSM. Other additional spatial information like GIS data about streets, railways and waterways can also be used as hint for the existence of biomass objects of interest in our definition.

Since the spectral unmixing works unsupervised, all abundance maps have to be manually checked if vegetation relevant for our objects of interest is represented. In Figure 4a and b two abundance maps indicating relevant biomass are illustrated where dark pixels correspond to 0 % and white pixel to 100 % of endmember membership of a pixel.

The vegetation map that is calculated from the LIDAR data is taken directly as biomass indicator, as illustrated in Figure 4c. Dark pixels correspond to no vegetation, white pixels represent the height of vegetation.

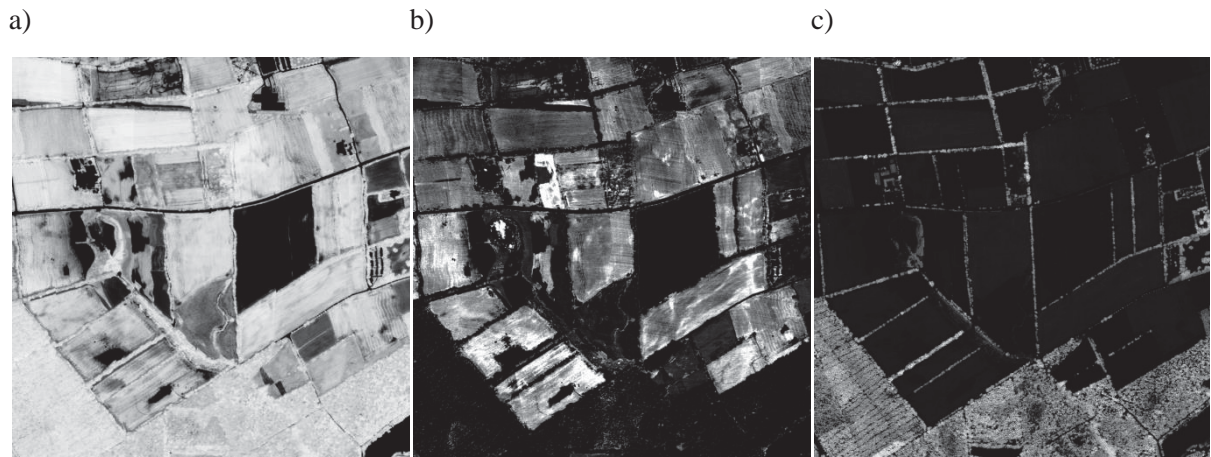


Figure 4: a) Endmember 4 representing vegetation and trees b) endmember 8 representing vegetation on fields c) vegetation height map.

5. Evaluation

The proposed approach is applied to test data from a test site in Germany, close to the city of Bottrop in North Rhine-Westphalia. The test site is located in a rural area with intensive agricultural use but contains also parts of a natural preserve.

To evaluate our approach, a vegetation map based only on the spectral unmixing results without use of height information is compared to a vegetation reference map based on LIDAR data. The vegetation map is a binary map considering all relevant abundance maps that are selected manually as described before. A pixel of the vegetation map is set to 1 if one or more abundance maps contain values > 50 % at this position.

The vegetation reference map also contains binary information of pixels containing vegetation larger than 0.3 m. Both maps are compared pixel-wise and 74.5 % of the reference vegetation pixels are recognized by spectral unmixing (cp. Figure 5). Considering the vegetation map 69.8 % of all pixel are correct vegetation compared to the reference, while 30.2 % are no vegetation in the reference.

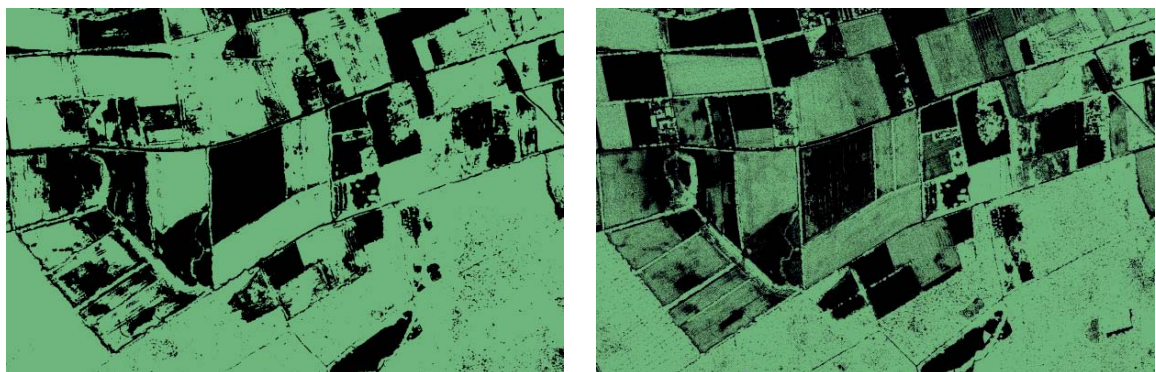


Figure 5: Vegetation map as result of spectral unmixing (left) vegetation reference map (right)

In terms of single biomass objects of interest, an evaluation is difficult because of rare reference data. The vegetation height map (Fig. 4c) is a very precise and valuable data source and nearly each

biomass landscape conservation object is contained in the data. By combining all information in a biomass potential map, to be done in a follow-up study, it will be possible to enable the detection of most landscape conservation objects of interest.

6. Conclusions

Our approach aims at mapping new alternative sources of biomass for energy production in contrast to common renewable energy sources. Exploring landscape conservation elements for energy production has a great potential. Some existing running pioneering projects work already with great success. To reduce data costs for the mapping task, a combination of Sentinel-2 satellite data, that will be freely provided in combination with height data, is proposed. Realistic sources to generate height information are widely available orthophotos and LIDAR data. Our result, a collection of biomass potential layers, builds a stable basis for a subsequent biomass amount estimation that is necessary to enable the harvest of biomass landscape elements.

Acknowledgements



The research is done within the joint research project BiomassMon (Phase 2) (<http://www.biomassmon.info/>) that is funded by the Federal Ministry of Economics and Technology (BMWi) via the German Aerospace Center (DLR e.V.) under the funding numbers 50EE1333, 50EE1334 and 50EE1335.

References

- [1] Ahamed, T., Tian, L., Zhang, Y., Ting, K.C., 2011: A review of remote sensing methods for biomass feedstock production, *Biomass and Bioenergy*, Volume 35, Issue 7, July 2011, Pages 2455–2469.
- [2] ASPRS LAS 1.4 Format Specification, November 14, 2011 http://www.asprs.org/a/society/committees/standards/LAS_1_4_r13.pdf
- [3] Bargiel, D., 2013. Capabilities of high resolution satellite radar for the detection of semi-natural habitat structures and grasslands in agricultural landscapes, *Ecological Informatics*, Volume 13, January 2013, Pages 9–16.
- [4] M. Drusch, U. Del Bello, S. Carlier, O. Colin, V. Fernandez, F. Gascon, B. Hoersch, C. Isola, P. Laberinti, P. Martimort, A. Meygret, F. Spoto, O. Sy, F. Marchese, P. Bargellini, 2012. Sentinel-2: ESA's Optical High-Resolution Mission for GMES Operational Services, *Remote Sensing of Environment*, Volume 120, May 2012, Pages 25-36.
- [5] Estornell, J., Ruiz, L.A., Velázquez-Martí, B., Hermosilla, T., 2012. Estimation of biomass and volume of shrub vegetation using LiDAR and spectral data in a Mediterranean environment, *Biomass and Bioenergy*, Volume 46, November 2012, Pages 710-721.
- [6] Forzieri, Giovanni, 2012. Satellite retrieval of woody biomass for energetic reuse of riparian vegetation, *Biomass and Bioenergy*, Volume 36, January 2012, Pages 432-438.
- [7] John H. Gruninger ; Anthony J. Ratkowski and Michael L. Hoke, 2004. "The sequential maximum angle convex cone (SMACC) endmember model", *Proc. SPIE 5425, Algorithms and Technologies for Multispectral, Hyperspectral, and Ultraspectral Imagery X*, 1 (August 12, 2004); doi:10.1117/12.543794; <http://dx.doi.org/10.1117/12.543794>.
- [8] Popescu, Sorin C., 2007. Estimating biomass of individual pine trees using airborne lidar, *Biomass and Bioenergy*, Volume 31, Issue 9, September 2007, Pages 646-655.
- [9] Segl, K.; Guanter, L.; Rogass, C.; Kuester, T.; Roessner, S.; Kaufmann, H.; Sang, B.; Mogulsky, V.; Hofer, S., 2012. "EeteS—The EnMAP End-to-End Simulation Tool," *Selected Topics in Applied Earth Observations and Remote Sensing, IEEE Journal of* , Volume 5, Number 2, Pages 522-530, April 2012